Empirical estimation of collapse capacity of post-mainshock buildings by generalized linear model

Ruiqiang Song[1], Shurong Fang[2], YueLi[1]

1. Department of Civil and Environmental Engineering, Michigan Technological University
2. Department of Mathematics and Computer Sciences, Fairfield University

Abstract

During earthquake events, numerous aftershocks are usually recorded following a mainshock and potentially cause further structural damage. This paper empirically estimates the collapse capacity of post-mainshock buildings using the generalized linear model (GLM). In this study, the inelastic spectral displacement is employed to quantify structural collapse capacity. The damage conditions for different buildings may differ greatly. It can significantly affect the collapse capacity and four damage states are considered here. A suite of 62 records with a broad range of earthquake ground motion characteristics are selected to determine collapse capacity by incremental dynamic analysis. The analysis is based on a nonlinear SDOF system and a typical 4-story steel framed building using deterioration models. A GLM of four parameters including the structural fundamental period, frequency content, duration, and damage state, is proposed to predict the collapse capacity. The maximum likelihood estimates of coefficients are determined by the iterative procedure. This research will facilitate the estimation of structural collapse capacity, and improve the current evaluation and design practice.

Keywords: generalized linear model, empirical estimation, collapse capacity

Introduction

During earthquake events, numerous aftershocks are usually recorded following a mainshock. They potentially cause further damage of post-mainshock buildings, pose a significant risk to life safety, hamper reoccupation and restoration of buildings, and increase seismic loss (Li et al., 2014). About 90 aftershocks with magnitudes 5.0 or greater are recorded in the 24 hours after the 2010 M8.8 Chile earthquake on February 27(USGS, 2010). The Great Tohoku earthquake on March 11, 2011, was followed by appropriate 588 aftershocks with moment magnitudes of 5.0 or greater in Japan (USGS, 2011).The M8.6 Indonesia earthquake on April 11, 2012, triggered many strong aftershocks with the largest measured at M8.2 in two hours (USGS, 2012).The ground motion characteristics of aftershocks may be remarkably different from those of mainshock due to the difference of occurrence mechanisms. Hence the accurate evaluation of the seismic behavior of post-mainshock buildings needs to account for aftershock hazard and its characteristics.

As ground motion characteristics (e.g., spectral shape, duration, and frequency content) may significantly affect the seismic behavior of buildings, it is required to consider the features of ground motion to accurately estimate the collapse capacity of a building subjected to earthquake records. Since the influence degree of the duration depends on many factors, such as the definition of duration, the seismic demand parameter, damage metric, and the structural nonlinear property, the effect of seismic duration on structural response is still a topic worth further investigation (Hancock & Bommer, 2006). Both experimental testing results of reinforced concrete and steel frames and analytical studies adopting the cumulative damage measures have demonstrated that the duration of ground motion or the number of loading cycles is positively correlated to structural damage (Chai, 2005; Dutta & Mander, 2001; Mander et al., 1995). van de Lindt and Goh (2004) found that seismic duration has a significant impact on structural reliability and proposed a duration effect factor to measure the effect of duration on reliability. Raghunandan and Liel (2013) investigated the effect of duration on collapse of reinforced concrete buildings with different structural properties and concluded that the collapse capacities of concrete structures with deterioration were greatly influenced by the ground motion duration.

Frequency content of ground motion may greatly influence the seismic response of buildings. Structural dynamic response and seismic forces can be significantly enhanced when the frequency content closely matches the natural periods of an elastic building (Chopra, 2007). Although a response spectrum provides the comprehensive information of frequency content, it is more convenient to characterize frequency content by a scalar parameter from an engineering practice perspective. Past studies have proposed several scalar frequency content parameters to investigate the influence of frequency content on the seismic behavior of buildings. Rathje et al. (1998) proposed the mean period T_m to measure the frequency content of ground motion, which is defined as the mean period of the Fourier amplitude spectrum (FAS) in a specified frequency range. Kumar et al. (2011) found that for single degree of freedom (SDOF) systems when the ratio of T_1 to T_m is lower than one the seismic displacement is amplified, while for multiple degree of freedom (MDOF) systems when T_m closely matches the higher mode periods the base shear and maximum story drift profile are significantly affected by structural modes. Kumar et al. (2013) found that the ratio of T_1 to T_m and the behavior factor have a remarkable influence on the global drift.

The effect of characteristics of ground motion records on the structural collapse is not well understood, especially the effect of aftershock features on post-mainshock collapse of buildings. This paper investigates the influence of characteristics of ground motion on collapse capacity for both post-mainshock SDOF and MDOF steel building models, and then estimates the post-mainshock collapse capacity using the generalized linear model (GLM). The structural analytical models are simulated by using the modified Ibarra-Krawinkler hysteretic model to capture the key structural degradation of strength and stiffness along with destabilizing effects of gravity loads. Incremental dynamic analysis was carried out to determine the structural collapse capacity based on a set of 62 aftershock records with varying characteristics. A generalized linear modeling regression technique was used to estimate the structural collapse capacity measured in terms of inelastic spectral displacement. This research will facilitate the estimation of structural collapse capacity, and improve the current evaluation and design practice.

Ground motion duration and frequency content

Many scalar parameters have been proposed in the literature to measure the ground motion duration. The 5-95% significant duration (D_s), defined as the interval of the times at which 5 and 95 percent of the Arias intensity of the ground motion are accumulated, is adopted in this study, since it has been recommended and used in a number of past studies (Aris, 1970). The Arias intensity (*AI*) which represents the integral over the seismic time of the square of the acceleration time history can be expressed as:

$$AI = \frac{\pi}{2g}\int_0^T a^2(t)dt \qquad (1)$$

where $a(t)$ is the ground motion acceleration, g is the gravity acceleration, and T is the total recorded time of a ground motion. Since D_s accounts for the seismic duration over which 90% of the total energy is accumulated, it represents the time length of the strongest part of ground motion.

Frequency content of ground motion is measured by the mean period T_m in this study. T_m is calculated by the weighted mean periods of the Fourier Amplitude Spectrum in a specific range of frequency. It can be mathematically expressed as (Rathje et al., 1998):

$$T_m = \frac{\sum_i C_i^2 \times \frac{1}{f_i}}{\sum_i C_i^2} \text{for } 0.25\text{Hz} \le f_i \le 20\text{Hz}, \text{with } \Delta f \le 0.05\text{Hz} \qquad (2)$$

Where f_i is the discrete fast Fourier transform (FFT) frequency in the range of 0.25 to 20 Hz, C_i is the Fourier amplitude coefficient corresponding to the frequency f_i, which is mutually independent, and Δf is the frequency interval for which the FFT is performed. To obtain a stable value of T_m, Rathje et al. (1998) suggested that the value of Δf should be smaller than 0.05 Hz. Rathje et al. (2004) demonstrated that T_m is a stable and reliable indicator of frequency content and it works well to distinguish the frequency content of strong ground motions.

Figure 1 shows the values of D_s and T_m for a mainshock-aftershock sequence, which was recorded at the CHY014 station from the 1999 Chi-Chi earthquake. The acceleration time history of the seismic sequence is shown in Figure 1 (a). Fig 1 (b) illustrates the comparison of the energy that accumulates over time between the mainshock and the aftershock. The Fourier Amplitudes corresponding to each frequency for the mainshock and the aftershock are shown in Fig 1 (c).

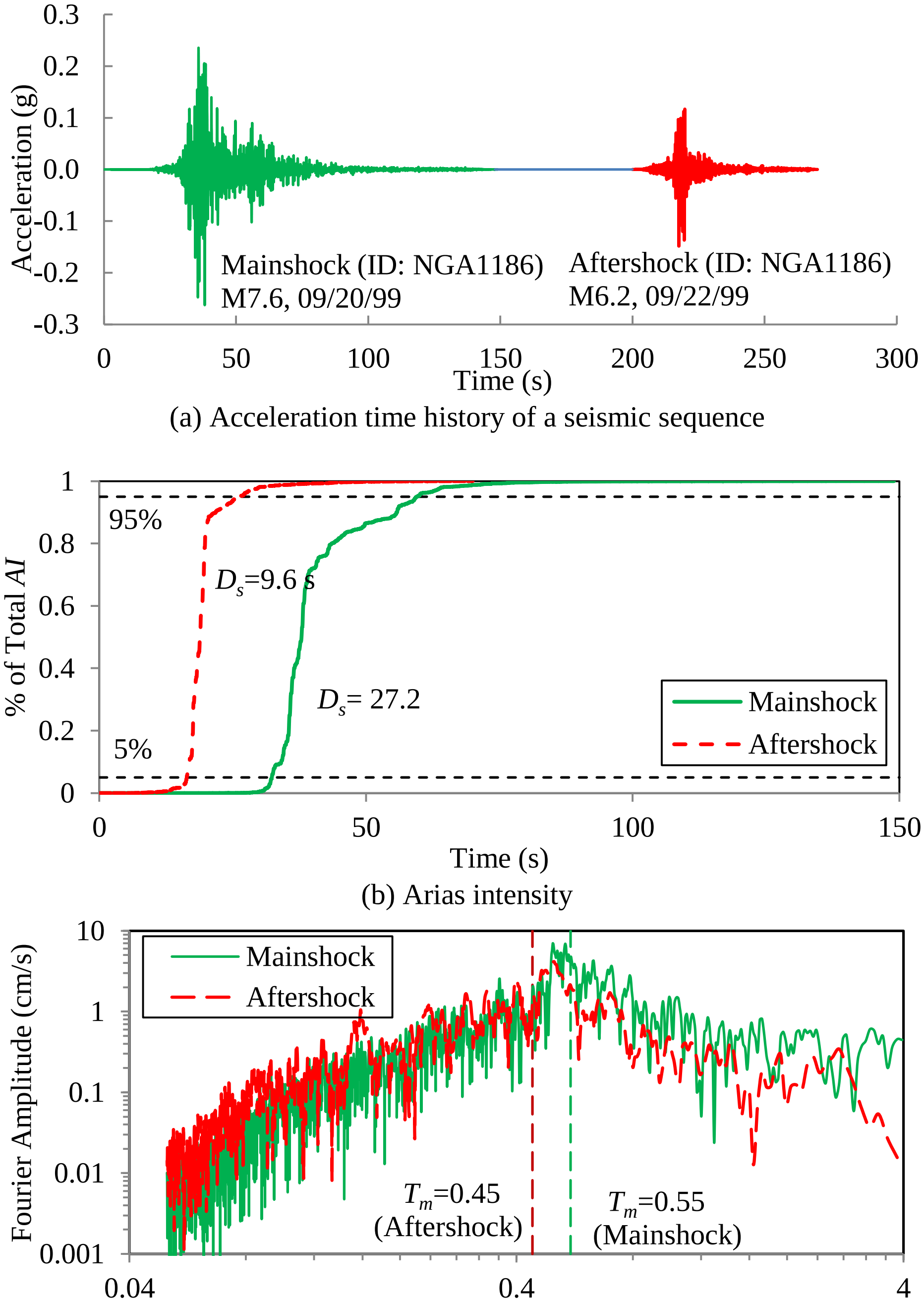

(a) Acceleration time history of a seismic sequence

(b) Arias intensity

(c) Fourier Amplitude Spectrum

Figure 1. D_s and T_m for a mainshock-aftershock sequence recorded at the CHY014 station from the 1999 Chi-Chi Earthquake

Mainshock-aftershock ground motion database

The mainshock-aftershock sequences in this study are obtained from the Pacific Earthquake Engineering Research Center (PEER) Next Generation Attenuation database (PEER, 2011) according to the following criteria: (1) the magnitude moment of mainshocks and aftershocks are equal to or greater than M5.0; (2) the peak ground acceleration (PGA) of horizontal components of ground motions are greater than 0.05 g; (3) only far-field ground motions are selected to avoid the effect of near site or rupture directivity; and (4) the acceleration sensors are installed on the free field or low-height buildings to avoid the influence of soil-structural interaction.

Under these criteria, 62 seismic sequences were selected from nine earthquake events with D_s ranging from 2.28 - 87.42 s and T_m varying between 0.19 - 1.29 s. The list of the selected seismic records and main parameters are present in Table 1. The spectral shape of ground motion is not considered in the selection process since the ground motion intensity is measured by the inelastic spectral displacement (S_{di}).

Table 1. Mainshock-aftershock sequences selected from PEER database

Earthquake name	Date	Time	Magnitude	Mechanism	Number of sequences
Chi-Chi, Taiwan	09/20/99	9:20	7.6	Reverse-Oblique	15
	09/20/99	18:03	6.2	Reverse	
	09/20/99	21:46	6.2	Strike-Slip	
	09/22/99	0:14	6.2	Reverse	
	09/25/99	23:52	6.3	Reverse	
Coalinga	05/02/83	23:42	6.4	Reverse	7
	05/09/83	2:49	5.1	Reverse	
	07/22/83	2:39	5.8	Reverse	
Friuli, Italy	05/06/76	20:00	6.5	Reverse	5
	09/15/76	3:15	5.9	Reverse	
Imperial Valley	10/15/79	23:16	6.5	Strike-Slip	6
	10/15/79	23:19	5.0	Strike-Slip	
Irpinia, Italy	11/23/80	19:34	6.9	Normal	7
	11/23/80	19:35	6.2	Normal	
Livermore	01/24/80	19:00	5.8	Strike-Slip	5
	01/27/80	2:33	5.4	Strike-Slip	
Mammoth Lakes	05/25/80	16:34	6.1	Normal-Oblique	5
	05/25/80	16:49	5.7	Strike-Slip	
	05/25/80	19:44	5.9	Strike-Slip	
Northridge	1/17/94	12:31	6.7	Reverse	8
	01/17/94	12:32	5.9	Reverse-Oblique	
	03/20/94	21:20	5.3	Reverse	
Whittier Narrows	10/01/87	14:42	6.0	Reverse-Oblique	4
	10/04/87	10:59	5.3	Reverse-Oblique	

Structural Models and Analysis

To explore the post-mainshock collapse capacity of buildings accounting for characteristics of aftershocks, nonlinear dynamic analysis is carried out for both SDOF and MDOF systems with deterioration models. The fundamental period of the SDOF system in this study is 0.85 s and the MDOF system is represented by a modern code-conforming four-story steel moment resistant frame building in Los Angeles (Lignos & Krawinkler, 2009). The design of the four-story office building was in accordance with the 2003 International Building Code (ICC, 2003), the 2002 Minimum Design Loads for Buildings and Other Structures (ASCE-7, 2002), and the 2005 American Institute of Steel Construction seismic provisions (AISC, 2005). Figure 2 shows the lateral steel moment-resisting frame in the East-West (EW) direction and the first three modal periods are 1.32, 0.39, and 0.19 s, respectively. To verify the analytical sidesway collapse of the frame, two 1:8 scale model frames were built and tested up to collapse on the shaking table at the NEES facility at the State University of New York at Buffalo (Lignos & Krawinkler, 2009).

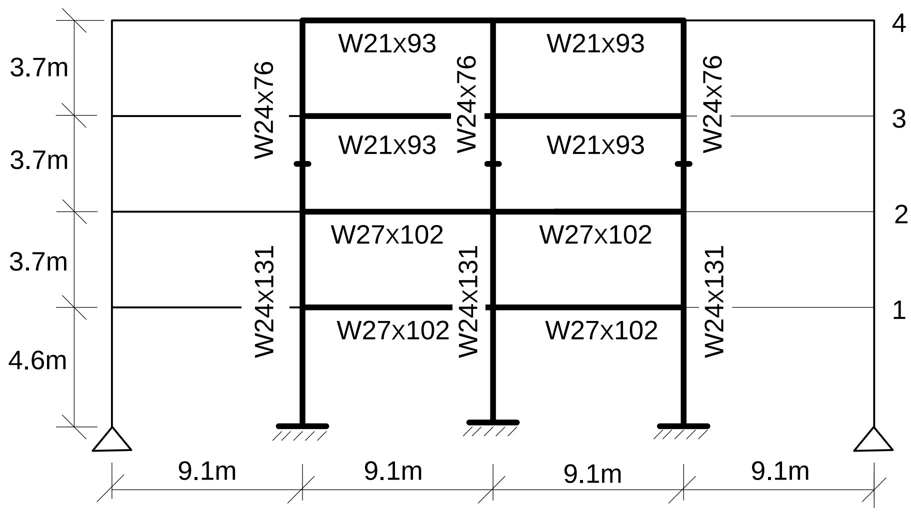

Figure 2. Four-story steel building

The OpenSees software developed by PEER was used to simulate the analytical models (OpenSees, 2013). To accurately simulate the seismic behavior to the collapse of buildings, the key degradation properties of the structural components are required to be captured in the nonlinear analytical models. The structural nonlinear behavior is simulated by a concentrated plasticity model, which consists of elastic beam-column elements connected by zero length elements to serve as the plastic hinge rotational spring (Eads et al., 2013; Lignos et al., 2011). The plastic hinge rotational spring is modeled by the modified Ibarra-Krawinkler hysteretic model, which accounts for rules for stiffness and strength deterioration (Lignos & Krawinkler, 2009). P-Delta effects are considered by linking a leaning column carrying gravity loads to the frame, which is modeled as beam-column elements jointed by zero length rotational spring elements with very small stiffness.

Incremental dynamic analysis (IDA) was applied to determine the collapse capacities of the buildings. An ensemble of ground motion records are used in an IDA to account for record-to-record variability and each record is scaled to multiple seismic intensity levels to force the structure through the entire range of structural behavior, from elastic to inelastic and finally to the structural collapse (Vamvatsikos & Cornell, 2002).

In this study, inelastic spectral displacement S_{di} is used to measure the seismic intensity because it is capable of representing the ground motion intensity, spectral shape effect, and elongated period (Tothong & Luco, 2007). S_{di} is calculated using a bilinear SDOF oscillator with a 5% post-yield hardening stiffness ratio and a 5% viscous damping ratio based on the structural fundamental period T_1 and the building-specific yield displacement d_y. Due to the yielding and elongated period of oscillator, S_{di} implicitly captures the spectra shape effect of the elongated period greater than T_1 which results from the structural damage. Accounting for ground motion intensity and spectral shape, S_{di} is efficient, sufficient, and has the scaling robustness to reduce record-to-record variability in the structural demands (Tothong & Luco, 2007).

Collapse capacity of post-mainshock buildings

Structural collapse capacity of buildings in this study is quantified by the inelastic spectral displacement S_{di} at the seismic intensity level that the global dynamic instability begins to occur. A larger S_{di} at collapse represents the building has a better performance to resist seismic hazard. The structural collapse is mainly attributed to the P-Delta effects, accumulated damage, and strength and stiffness degradation of the components, etc. (Li et al., 2014).

The damage conditions for post-mainshock buildings may differ significantly depending on the variation of seismic intensity and the characteristics of the seismic resistance of the building. When a post-mainshock building sustains severe damage, the structural post-mainshock collapse capacity could be significantly reduced. In this study, four typical post-mainshock damage states are taken into account, including the undamaged state (DS_0), and three damage states (DS_1, DS_2 and DS_3) defined in ATC-58 (ATC-58, 2012). For a steel ductile moment resisting, the median peak interstory drifts of 1.5%, 2.7% and 4.1% correspond to the damage states DS_1, DS_2 and DS_3, respectively. The four damage states can be termed as none, minor, moderate, and severe damage for buildings. In this study, 62 aftershock records listed in Table 1 were used in the IDA to investigate the influence of aftershock characteristics on the collapse capacity of post-mainshock buildings with different damage states.

Figure 3 and 4 present the relationship among collapse capacity S_{di}, duration D_s and mean period T_m for the SDOF structure and the 4-story building with four damage states, respectively. Each "circle" marker in Figure 3 and 4 represents a collapse S_{di} determined by IDA for each ground motion. As shown in Figure 3, it is noted that the collapse capacities S_{di} of buildings with different damage states usually decrease as D_s and T_m increases. As the damage level increases, the collapse capacity of buildings is significantly decreased.

In order to estimate collapse capacity of post-mainshock buildings, a multivariate regression based on generalized linear model (GLM) framework (Fox, 2008) is used to quantify the influence of frequency content, duration, and damage state on the structural collapse capacity. The generalized linear model includes three components: the probability distribution from the exponential family, linear predictor, and a link function relating the linear model to the response variable. A function of four parameters including the structural fundamental period T_1, the duration D_s, the frequency content T_m, and damage state DS, is proposed to estimate the structural collapse capacity S_{di} using GLM. The function is expressed in Eq. (3), where ε is the error term.

$$S_{di} = f(T_1, D_s, T_m, DS) + \varepsilon \tag{3}$$

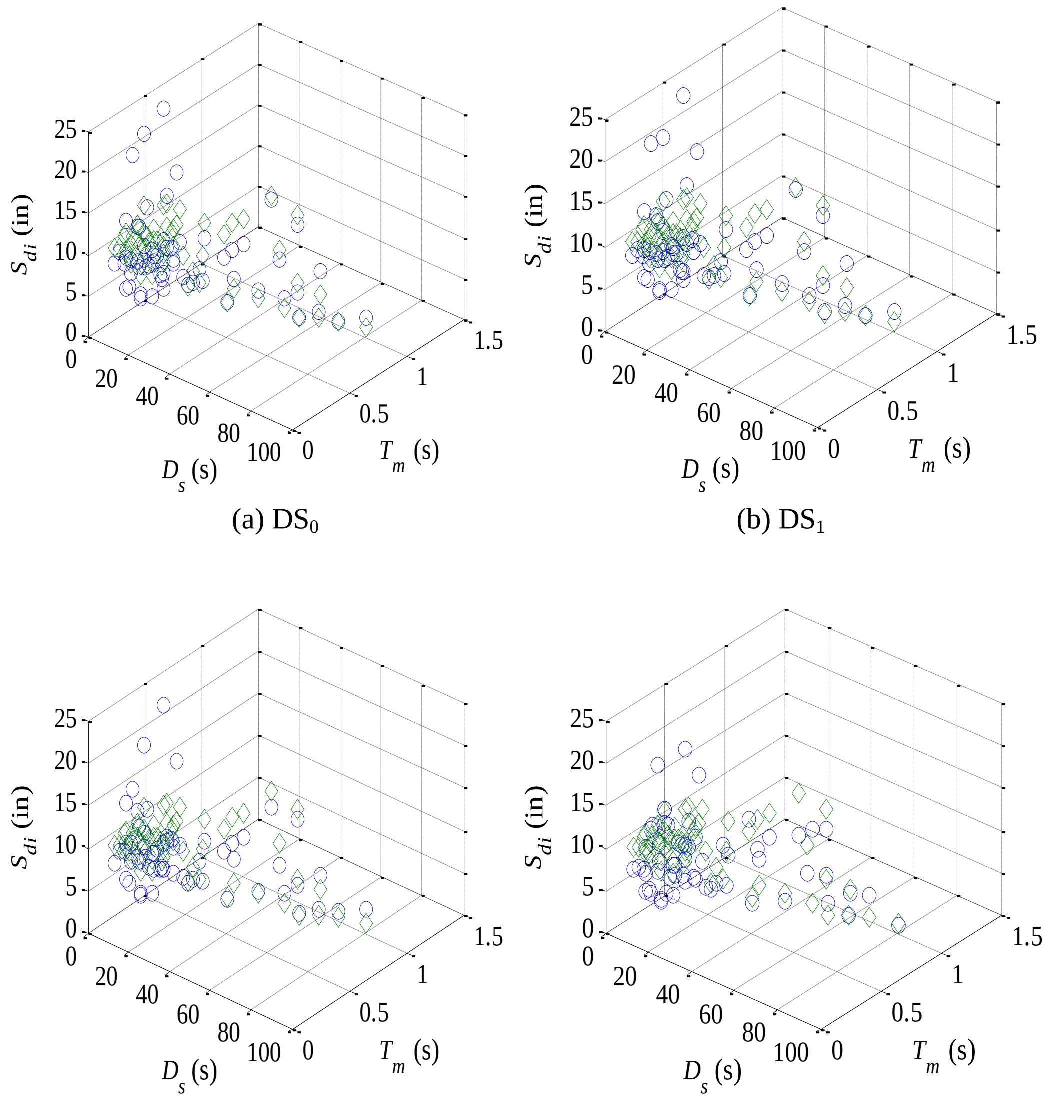

(a) DS_0 (b) DS_1

(c) DS_2 (d) DS_3

Figure 3. Variation of collapse S_{di} with T_m and D_s for the SDOF system at four damage states (Circle: Analysis result and Diamond: Fitted GLM model)

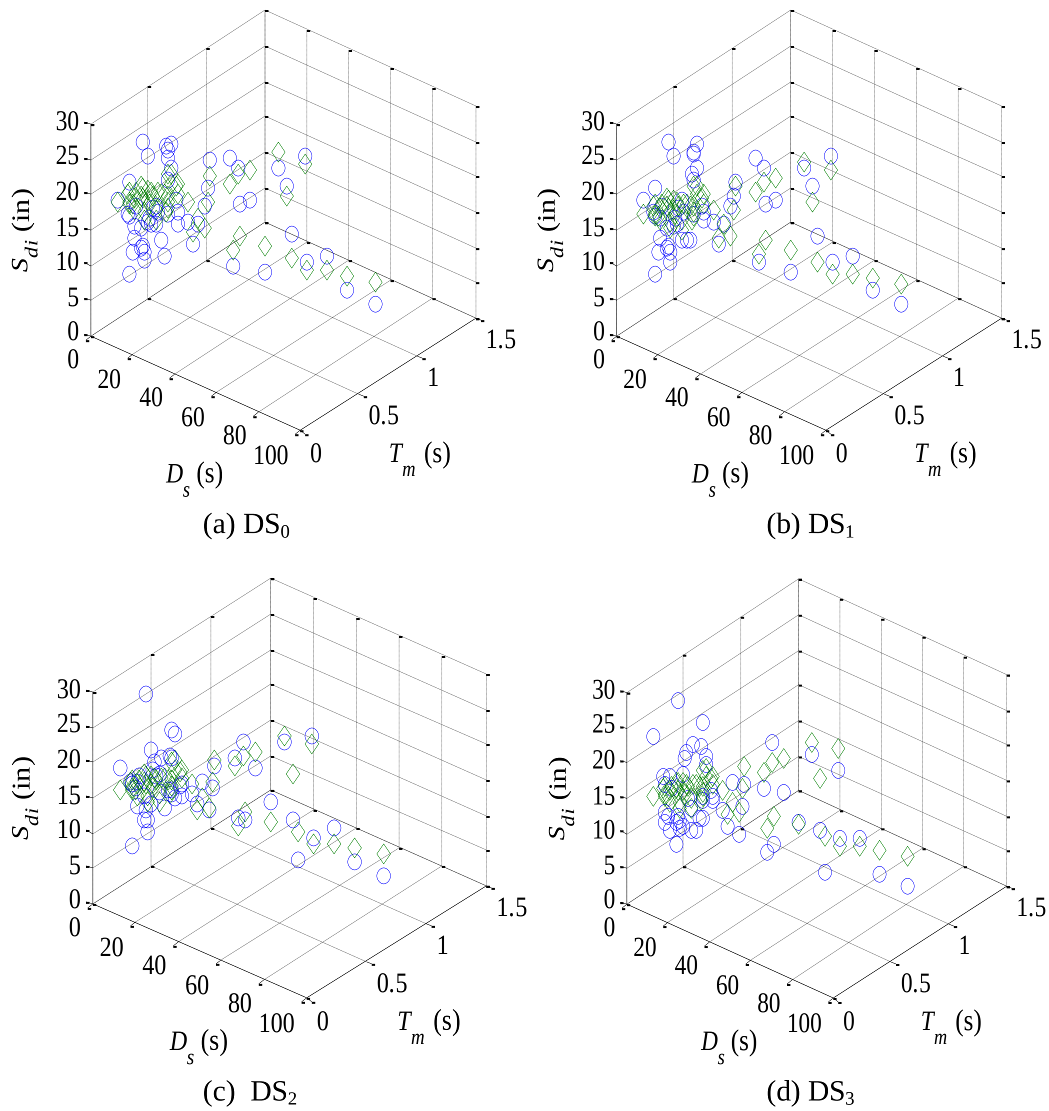

Figure 4. Variation of collapse S_{di} with T_m and D_s for the 4-story building at four damage states (Circle: Analysis result and Diamond: Fitted GLM model)

Since structural collapse capacity typically follows a lognormal distribution, the response variable Y is assumed to follow the gamma distribution, which can match the shape of lognormal distribution by adjusting the shape and scale parameters. An inverse link function for the response variable Y is expressed as:

$$E(S_{di}) = g^{-1}(X^T\beta) = \frac{1}{(1, T_1, T_m, D_s, DS)^T\beta} \tag{5}$$

The nonlinear variation of collapse S_{di} with the four parameters can be captured by the inverse link function. The mean of collapse S_{di} can be estimated by a constant shape parameter and varied scaled parameter capturing the variation of collapse S_{di}. The variance of the gamma distribution is proportional to the square of the mean (Raghunandan & Liel, 2013).

Table 2. Fitted GLM model parameters

Model parameter	β	Standard error	p value
Intercept	2.86E-02	6.04E-03	3.1E-06
Fundamental period T_1	-1.91E-02	4.69E-03	5.6E-05
Duration D_s	2.95E-03	4.12E-04	3.2E-12
Mean period T_m	-5.12E-02	1.48E-02	5.7E-04
Damage State *DS*	5.01E-02	1.84E-02	6.7E-03
$D_s \times T_1$	-2.17E-03	3.15E-04	1.8E-11
$T_m \times T_1$	3.81E-02	1.14E-02	9.5E-04

The GLM package in software R (R, 2013) is used to obtain the regression coefficients in the inverse link function by determining the maximum likelihood estimates in the iterative procedure. The different combination of T_1, D_s, T_m, *DS*, the multiplicative interaction parameters $T_m \times T_1$, and $D_s \times T_1$ are fitted in the GLM. In the regression analysis, the response variable refers to 496×1 vector of collapse S_{di} for 2 buildings and 62 ground motions, and the size of predictor variable matrix is 496× 4. By minimizing the predicted residual sum of squares, the fitted GLM model in Eq. (6) shows that the T_1, D_s, T_m, *DS*, and interaction term $D_s \times T_1$ and $T_m \times T_1$ are important for predicting the mean of collapse S_{di}. Figure 3 and 8 show the predicted mean collapse capacity S_{di} for the SDOF system and the 4-story building from the fitted GLM model, respectively. Each "Diamond" marker indicates a collapse S_{di} predicted from Eq. (6).

$$E[S_{di}] = (2.86 \times 10^{-2} - 1.91 \times 10^{-2} * T_1 + 2.95 \times 10^{-3} * D_s - 5.12 \times 10^{-2} * T_m + 5.01 \times 10^{-2} * DS - 2.17 \times 10^{-3} * D_s \times T_1 + 3.81 \times 10^{-2} * T_m \times T_1)^{-0.5} \quad (6)$$

The statistical significance of the fitted GLM model parameters (β) is tested by using the Analysis of Variance in R (R, 2013). The β values and the standard error used in hypothesis testing are summarized in Table 2. The β values are assumed to be zero in the null hypothesis. The null hypothesis can be rejected if the corresponding p value is less than the 5% significance value. The results of testing listed in Table 2 show that all the p values are close to zero and the null hypothesis should be rejected. Therefore, each of the selected predictors: T_1, D_s, T_m, DS, $D_s \times T_1$ and $T_m \times T_1$ is important.

Conclusions

This study investigates the effect of ground motion characteristics and damage state on the post-mainshock collapse capacity. The results demonstrate that the ground motion characteristics play a significant role in the structural collapse capacity whether for a simplified SDOF or more complex MDOF model. A post-mainshock building with a higher damage state may have a lower collapse capacity when it is subjected to an aftershock with longer duration and higher mean period. Thus, a vector of intensity measure capable of reflecting the ground motion intensity, duration, and frequency content may provide a better estimation of structural collapse capacity than a scalar intensity parameter. Based on the generalized linear model, the study proposes an empirical estimation equation of mean value of structural post-mainshock collapse capacity. Given the features of aftershocks and structural damage states, the mean post-mainshock collapse capacity can be empirically estimated. More investigations of post-mainshock collapse of buildings are needed to account for varying structural properties, failure mechanisms, hysteretic models, buildings types, etc. In addition, variation of post-mainshock collapse capacity of buildings is needed to incorporate into the framework of the performance-based earthquake engineering.

Acknowledgements

The research described in this paper was supported, in part, by the National Science Foundation (NSF) Division of Civil, Mechanical, and Manufacturing Innovation (CMMI) under Grant No. CMMI-1100423. The support is gratefully acknowledged. However, the writers take sole responsibility for the views expressed in this paper, which may not represent the position of the NSF or their respective institutions.

References:

AISC. (2005). *Seismic Provisions for Structural Steel Buildings, Including Supplement No. 1*. Chicago (IL): American Institute of Steel Construction (AISC).

Aris, A. (1970). *A measure of earthquake intensity, seismic design for nuclear power plants* Cambridge, MA: MIT Press.

ASCE-7. (2002). *Minimum design loads for buildings and other structures*. Reston (VA): Structural Engineering Institute (SEI).

ATC-58. (2012). *Seismic Performance Assessment of Buildings, Volume 1 – Methodology*. Redwood City, CA: Applied Technology Council.

Chai, Y. (2005). Incorporating low-cycle fatigue model into duration-dependent inelastic design spectra. *Earthquake Engineering & Structural Dynamics, 34*(1): 83-96.

Chopra, A. K. (2007). *Dynamics of structures: Theory and applications to earthquake engineering* (Third ed.). Upper Saddle River, NJ: Prentice Hall.

Dutta, A., & Mander, J. (2001). Energy based methodology for ductile design of concrete columns. *Journal of Structural Engineering, 127*(12): 1374-1381.

Eads, L., Miranda, E., Krawinkler, H., & Lignos, D. G. (2013). An efficient method for estimating the collapse risk of structures in seismic regions. *Earthquake Engineering & Structural Dynamics, 42*(1): 25-41.

Fox, J. (2008). *Applied regression analysis and generalized linear models*. Los Angeles, CA: Sage Publications.

Hancock, J., & Bommer, J. J. (2006). A state-of-knowledge review of the influence of strong-motion duration on structural damage. *Earthquake Spectra, 22*(3): 827-845.

ICC. (2003). *2003 International Building Code*. Falls Church (VA): International Code Council.

Kumar, M., Castro, J., Stafford, P., & Elghazouli, A. (2011). Influence of the mean period of ground motion on the inelastic dynamic response of single and multi degree of freedom systems. *Earthquake Engineering & Structural Dynamics, 40*(3): 237-256.

Kumar, M., Stafford, P., & Elghazouli, A. (2013). Influence of ground motion characteristics on drift demands in steel moment frames designed to Eurocode 8. *Engineering Structures, 52*: 502-517.

Li, Y., Song, R., & van de Lindt, J. W. (2014). Collapse Fragility of Steel Structures

Subjected to Earthquake Mainshock-Aftershock Sequences. *Journal of Structural Engineering, In press*.

Lignos, D. G., & Krawinkler, H. (2009). *Sidesway Collapse of Deteriorating Structural Systems Under Seismic Excitations.* (Ph.D.), Stanford University, John A. Blume Earthquake Engineering Center.

Lignos, D. G., Krawinkler, H., & Whittaker, A. S. (2011). Prediction and validation of sidesway collapse of two scale models of a 4-story steel moment frame. *Earthquake Engineering & Structural Dynamics, 40*(7): 807-825.

Mander, J. B., Pekcan, G., & Chen, S. S. (1995). Low-cycle variable amplitude fatigue modeling of top-and-seat angle connections. *Engineering Journal, 32*(2): 54-62.

OpenSees. (2013). The Open System for Earthquake Engineering Simulation. Retrieved September 05, 2013, from http://opensees.berkeley.edu

PEER. (2011). Pacific Earthquake Engineering Research Center PEER Strong Motion Da tabase. Retrieved October 01, 2011, from http://peer.berkeley.edu/peer_ground_motion_database/spectras/16318/unscaled_searches/new

R. (2013, 2013). The R project for statistical computing. Retrieved 1 October, 2013, fro m http://www.r-project.org/

Raghunandan, M., & Liel, A. B. (2013). Effect of ground motion duration on earthquake-induced structural collapse. *Structural Safety, 41*: 119-133.

Rathje, E. M., Abrahamson, N. A., & Bray, J. D. (1998). Simplified frequency content estimates of earthquake ground motions. *Journal of Geotechnical and Geoenvironmental Engineering, 124*(2): 150-159.

Rathje, E. M., Faraj, F., Russell, S., & Bray, J. D. (2004). Empirical relationships for frequency content parameters of earthquake ground motions. *Earthquake Spectra, 20*(1): 119-144.

Tothong, P., & Luco, N. (2007). Probabilistic seismic demand analysis using advanced ground motion intensity measures. *Earthquake Engineering & Structural Dynamics, 36*(13): 1837-1860.

USGS. (2010). Magnitude 8.8 - offshore Bio-bio, Chile. Retrieved April 05, 2012, from http://earthquake.usgs.gov/earthquakes/eqinthenews/2010/us2010tfan/#summary

USGS. (2011). Magnitude 9.0 - near the east coast of Honshu, Japan. Retrieved April 05, 2012, from http://earthquake.usgs.gov/earthquakes/eqinthenews/2011/usc0001xgp/#summary

USGS. (2012). Magnitude 8.6 - off the west coast of Northern Sumatra. Retrieved Jan 06, 2013, from http://earthquake.usgs.gov/earthquakes/recenteqsww/Quakes/usc000905e.php#summary

Vamvatsikos, D., & Cornell, C. A. (2002). Incremental dynamic analysis. *Earthquake Engineering & Structural Dynamics, 31*(3): 491-514.

van de Lindt, J. W., & Goh, G. (2004). Earthquake duration effect on structural reliability. *Journal of Structural Engineering, 130*(5): 821-826.